THE VECTOR EXPERIMENT FOR THE REXUS 7 AND 8 SOUNDING ROCKET

Steffen Jäkel, Konrad Makowka, Elias Breunig, Sebastian Colditz, Florian Aschauer, Sebastian Herzig, Christian Scharl, Joachim Müller, Markus Pietras, Andreas Fleischner

Technische Universität München, Institute of Astronautics, Boltzmannstr. 15, 85748 Garching, Germany
steffenjaekel@mytum.de, konrad.makowka@mytum.de, elias-breunig@mytum.de, sebastian.colditz@mytum.de, florian.aschauer@mytum.de, sebastian.herzig@mytum.de, christian.scharl@mytum.de, joachim.mueller@mytum.de, m.pietras@tum.de, a.fleischner@tum.de

ABSTRACT

This paper presents results and experiences gathered from the VECTOR (Verification of Concepts for Tracking and Orientation) experiment within the REXUS sounding rocket program. A novel dynamic spiral tracking (DST) concept for the tracking of fast-moving objects, such as sounding rockets, is introduced. The method is based on conical motion of the antenna around the vector to its anticipated target as well as the measurement and processing of the received signal strength from the rocket-borne radio transmitter.
In addition to the tracking experiment, a hardware implementation of an on-board real-time video compression system for space missions based on the CCSDS standard was tested. In order to meet the specified real-time compression performance, a FPGA hardware implementation was developed.

1. BEAM TRACKING ALGORITHM

1.1. Background and Tracking Schematic

The purpose of the Beam Tracking Algorithm (BTA) is the autonomous pointing of the receiving Lightweight Inter-Satellite Antenna (LISA) [1] to the fast moving rocket target, in order to ensure stable link conditions during the whole flight. The autonomous tracking method implemented within the VECTOR experiment is based on conical motion of the antenna around the vector to its anticipated target while measuring and processing the signal strength distribution on the cone. By calculating the direction of maximal signal strength, the center position of the next scanning cone is determined. The resulting behavior of the antenna motion, while following a moving target, can be described as a spiral movement and is therefore referred to as Dynamic Spiral Tracking (DST). While other tracking methods use supplementary expensive equipment, such as radar or electronic-beam forming for target determination, the developed tracking technology is solely based on measurement of the current signal strength in the main lobe direction of the receiver antenna. The tracking system's functionality was tested during the REXUS 7 flight without data transmission by utilizing the HF signal emitted by the REXUS Service Module [2] as a radio beacon and finally demonstrated successfully with downlink capabilities during the REXUS 8 flight.

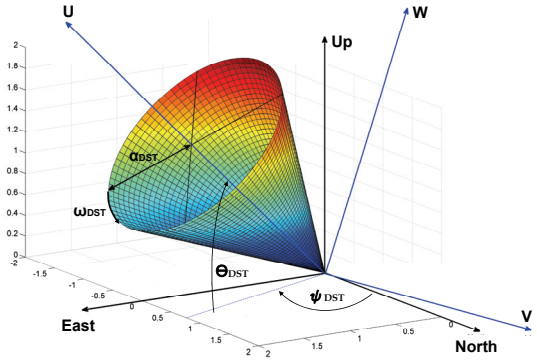

Figure 1: DST scanning cone with parameters and reference coordinate systems

1.2. Tracking Principle Description

A DST scanning cone is described by its opening angle α_{DST} and the angular velocity of the conical movement $\omega_{DST}=2\pi f_{DST}$. Fig. 1 depicts this while axis U is being collinear to the cones symmetry axis and points into the anticipated target direction. The North-East-Up (NEU) frame is inertially fixed to the earth's surface, while the UVW frame turns, following the attitude of the DST scanning cone. Additional to its opening angle and the conical motion angular velocity, the DST scanning cone is further defined by the current azimuth $\psi_{DST,k}$ and elevation $\theta_{DST,k}$ angles to its symmetry axis U.

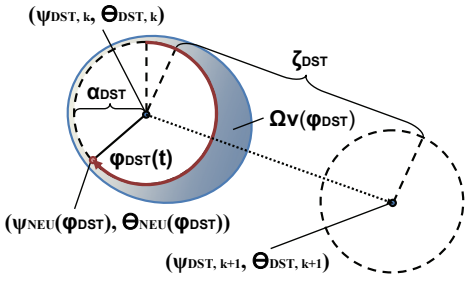

Figure 2: DST scanning cone parameters and transition

While the antenna carries out the conical movement, the received and appropriately filtered signal strength Ω_V on the cone is measured and correlated to the antenna

position, as shown in Fig. 2. After a completed circular motion, the direction of maximal signal strength is calculated. Applying an angular step $\zeta_{DST,k}$ in this direction creates the alternated angles $\psi_{DST,k+1}$ and $\theta_{DST,k+1}$ as the new center position for the next scanning cone.

Since the tracking algorithm is based on the signal variation due to the antenna's circular movement around the target, it is imperative to separate relevant signal fluctuation for tracking from disturbing signal deviation caused by the environment and system effects. The raw signal strength for tracking is especially overlaid with parasitic signal fluctuations due to unpredictable rocket rotation and background noise. The frequency to be extracted is equal to the DST frequency f_{DST}.

In addition to the tracking method described above, a backup system named auto-track using actual target azimuth and elevation data provided by Esrange's local posnet [2] was implemented. In case of appreciable deviation between current DST and posnet position, the center position is being set back to the posnet position. Applying this procedure allows continuing autonomous tracking after unstable tracking conditions and provides a data basis for after-flight evaluation of the tracking performance as explained in chapter 1.5.

1.3. Parameters Affecting Performance

The DST frequency f_{DST} determines the time span the antenna needs to complete one scanning motion. A higher DST frequency implies more scanning cones in the same amount of time and results in smaller angular step sizes $\zeta_{DST,k}$ after each cone. It is unlikely that the algorithm will provide an ideal antenna pointing after a single step. However, the repeated application of many steps will sum up to an adequate antenna pointing. It was shown in simulation and testing that a high DST frequency is desirable as assumed since it increases the number of alignment corrections.

The DST cone opening angle α_{DST} determines the magnitude in signal deviation during one scanning cone. It must be large enough to ensure a reliable acquisition of an unambiguous maximum signal strength direction. Furthermore, since a large cone angle leads to high angular deviations between the target and the antenna pointing direction, resulting in worse signal quality and larger dynamic forces on the system, it should be kept small. The DST angle was chosen with 3° as this outlines a fair trade-off for this specific application.

During the time of completion of one DST scanning cone, the rocket moves at an angle defined by its angular velocity times the interval for the DST circle. The step size ζ_{DST} must at least be equal to this value to allow the following for the rocket. It must also be limited to prevent antenna misalignment, creating superfluous oscillation around the optimal pointing vector to the target. Concepts including a dynamically adapted step size have been discarded due to lack of reliability. Simulations and extensive testing have shown that introducing a jump decision for the execution of the step ζ_{DST} based on a threshold in signal variance reduces the robustness of the tracking systems. Even though this procedure reduces the tracking systems oscillations around the optimal target alignment, it failed during some flight periods. Therefore, every time a scanning cone is completed, a new center position is being set with a predefined and time-dependant step-size. Nevertheless, a dynamical step-size adaptation is a promising option to improve the algorithm in future developments.

The use of an adequate filtering technique turned out to be a crucial factor for the tracking performance. This task is accomplished by several Butterworth-type IIR-filters. For each specific DST frequency chosen one pair of high-pass and low-pass filters was implemented.

1.4. Implementation

The tracking algorithm was implemented using a Matlab/Simulink xPC Target real-time simulation environment on a stand-alone machine that allowed fast and effective implementation.

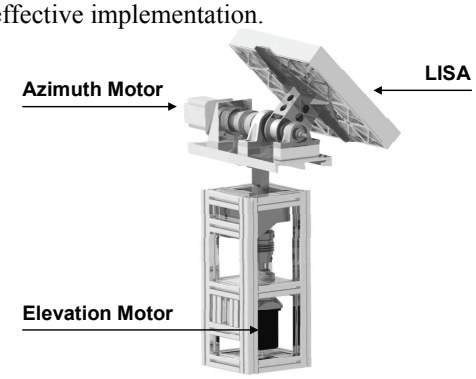

Figure 3: Antenna steering mechanism with LISA

The steering of LISA is done by a two dimensions of freedom (DOF) antenna mechanism as depicted in Fig. 3. The elevation axis is positioned on top of the azimuth axis, which has an important effect when describing the motors' dynamics in order to move the antenna conically.

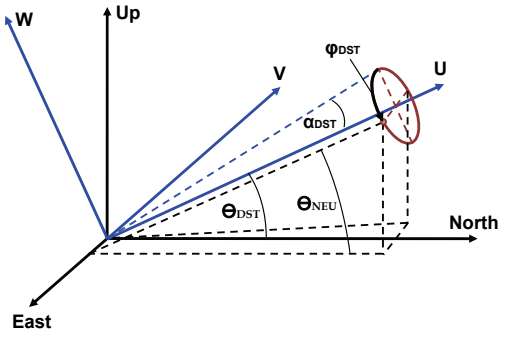

Figure 4: DST cone coordinate transformation

As shown in Fig. 4, the DST scanning cone coordinate system UVW is turned by its center azimuth ψ_{DST} and elevation θ_{DST} relative to the mechanism-fixed NEU frame. While the elevation axis movements do have full effect on the antenna's movement in this direction, depending on the current center elevation, only a fraction of the vertical azimuth movement is transferred to the antenna's change in azimuth. Taking this coordinate transformation into account, the actual motor positions for azimuth and elevation derive as follows (Eqs. 1-2).

$$\psi_{NEU} = \psi_{DST} + \arctan\left(\frac{\sin\varphi_{DST}}{\frac{1}{\tan\alpha_{DST}}\cos\theta_{DST} - \sin\theta_{DST}\cos\varphi_{DST}}\right) \quad (1)$$

$$\theta_{NEU} = \arctan\left(\frac{\sin\theta_{DST} + \cos\theta_{DST}\cos\varphi_{DST}\tan\alpha_{DST}}{\cos\theta_{DST} - \sin\theta_{DST}\cos\varphi_{DST}\tan\alpha_{DST}}\right) \quad (2)$$

The result of these relations can be seen in Fig. 5. Given a constant DST scanning cone opening angle, the actual motor movements increase significantly with rising DST center elevation θ_{DST}. Since the time for one DST circle stays the same, the motor's velocity and acceleration increase accordingly.

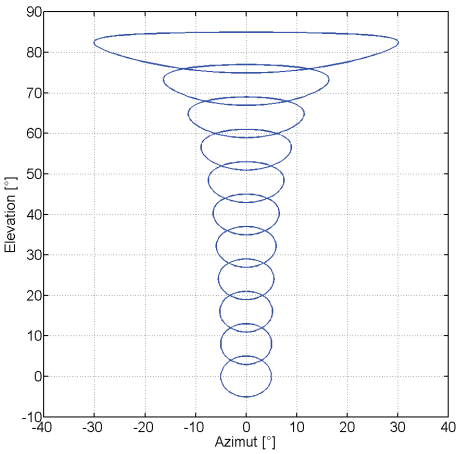

Figure 5: Resulting azimuth and elevation motor positions for a fixed opening angle α_{DST} and different DST center elevations θ_{DST}

In addition to this, the chosen motor configuration creates a singularity at 90° of elevation, which in this case, however, doesn't have an impact on the tracking performance, since the relative target elevation is limited to roughly 80°.

From the tracking algorithms point of view, a high cone scanning frequency is desirable, since it increases the algorithm's performance and ability to track fast-moving objects. One boundary with consideration to f_{DST} is the remaining amount of signal strength measurement points within one scanning circle. This is due to the fact that the sampling rate of the associated A/D converter is limited (1.2 kHz in this case). Another much more influential point is the dynamic force acting on the electric motor actuators, that are of course limited in their ability to endure torque without producing stepping mistakes. Those are not wanted, because they will result in an offset between the originally calibrated North-East-Up frame and the actual geographic North, creating artificial divergence between current and posnet position. Since the acceleration (leading to dynamic force) of the azimuth motor increases drastically at high elevations, a DST frequency between 1.6Hz at low and 1Hz at high elevation was implemented.

1.5. Results Gained from Both Rocket Flights

As mentioned above, an adequate filtering technique for extracting the signal variation due to the DST scanning motion is crucial for a successful beam tracking. However, the rocket's rotational frequency comes very close to the DST frequency at two instances during the flight. The first overlap takes places when the rocket's de-spin system is being activated approximately 70s after launch and the second one when the rocket re-enters the earth's atmosphere, tumbling severely. The second case especially implies significant difficulties for distinguishing the DST signal change from the rocket's rotation. In fact, it is not possible for the used filtering techniques to extract the DST signal when the rocket rotates with a frequency very close to the DST frequency. As anticipated, DST becomes worse due to the uncontrolled tumbling close to the DST frequency between 210s and 250s in-flight, leading to several auto-track activations. Unfortunately, there was an internal data dropout during the REXUS 8 flight after 250s for approximately 30s leading to an artificial auto-track activation from 250s to 280s, as can be seen in Fig. 7. Instead of following the rocket accurately as would have probably been the case, the antenna is set back on an outdated posnet position. One can see the important influence of the angular step size between two scanning circles in the REXUS 8 plot after 280s. The chosen step size was too small for this last flight phase and as a result, the antenna could not follow the rocket fast enough, even though the direction was correct. Therefore, future enhancements should strongly focus on an improved step-size management.

REXUS 7 tracking was quite successful as one can see in Fig. 6, generating only very few auto-track activations. At about 210s in-flight auto-track was activated as it had been predicted in previous simulations due to the rocket's rotational frequency coming close to the DST frequency. Furthermore, there had been an error of about 7° in the antenna's azimuth angle calibration towards north. One can see the effect in the REXUS 7 azimuth plot. The algorithm tries to align the antenna towards the rocket to compensate the initial azimuth orientation error. The posnet position data did not fit that pointing direction because of the

error in the north calibration. Therefore, the antenna was set back to the wrong posnet position by auto-track several times, especially in the last flight phase. Nevertheless, it is a satisfying result that the algorithm was able to correct the adjustment error autonomously.

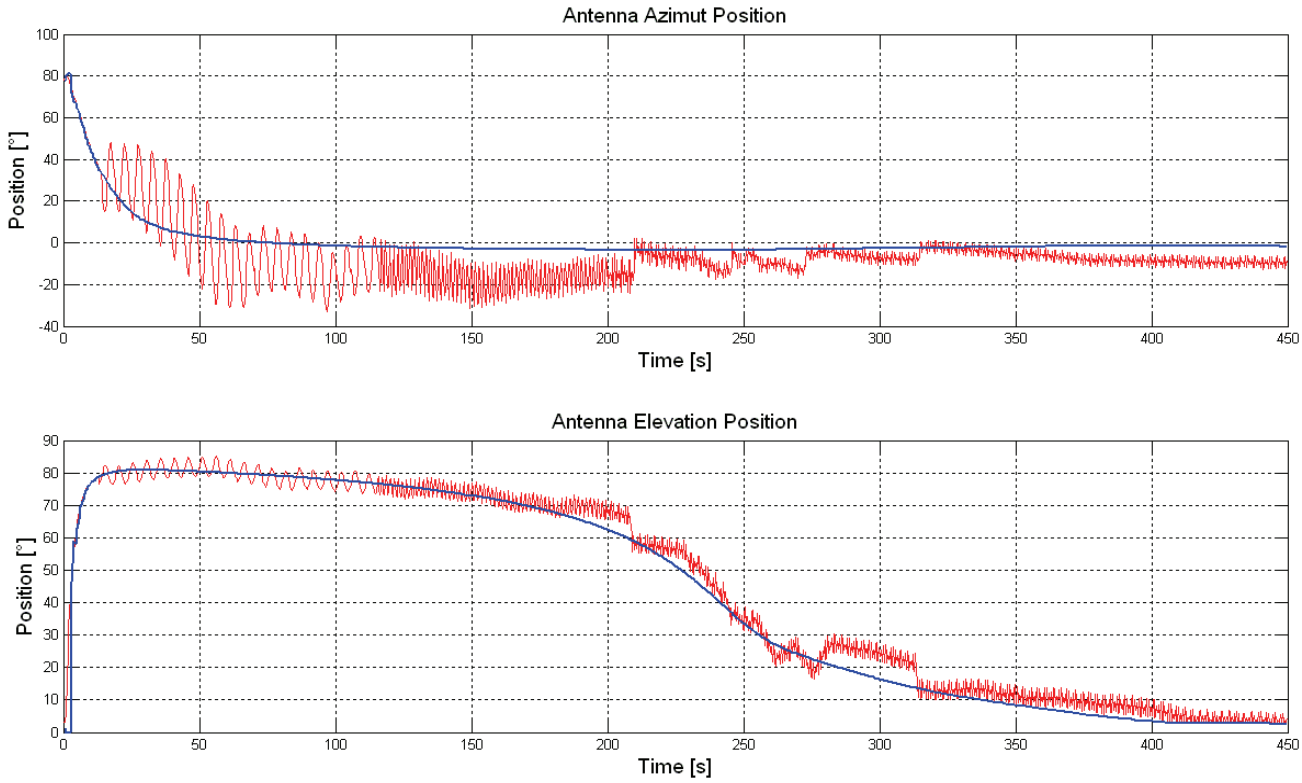

Figure 6: REXUS 7 tracking plot

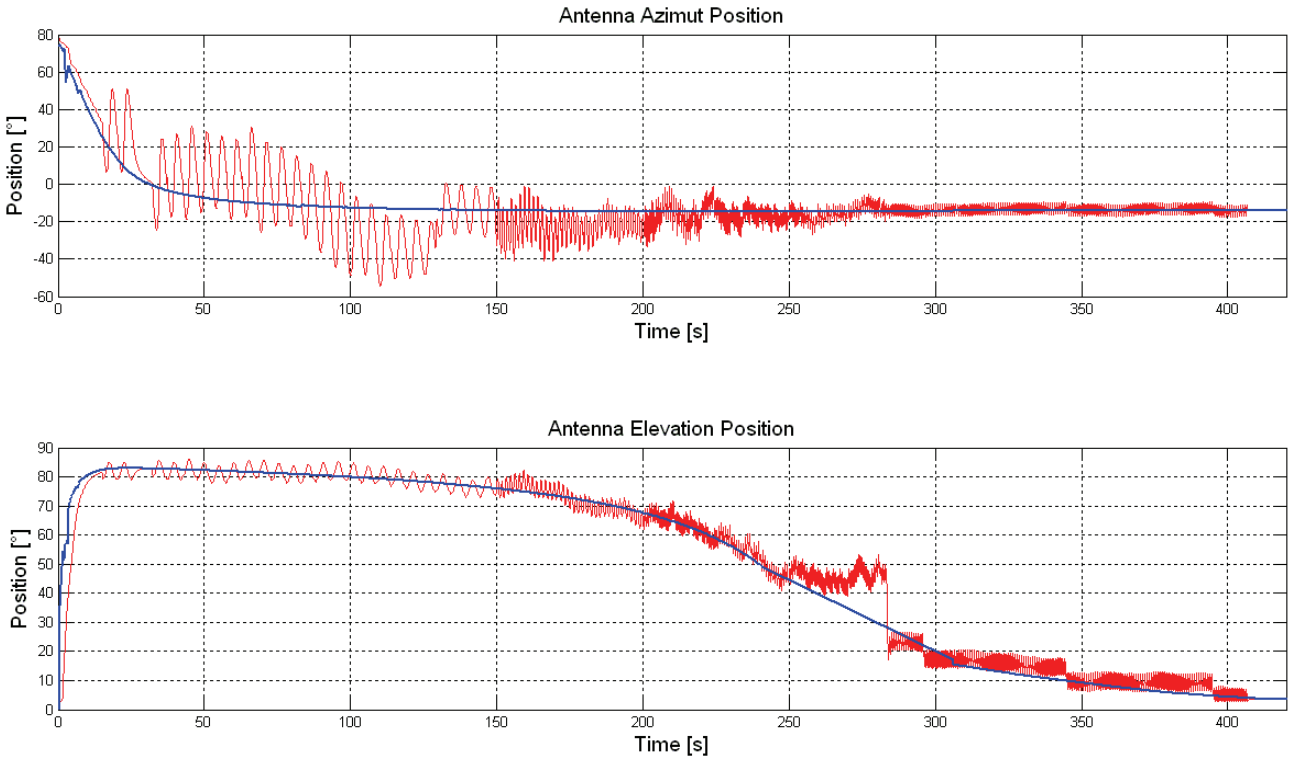

Figure 7: REXUS 8 tracking plot

2. SPACE SEGMENT SOFTWARE DEVELOPMENT WITH NI LABVIEW

2.1. Space Segment Components and Requirements

The VECTOR space segment's main goals were to provide a radio beacon to be tracked by the LISA antenna, to show the feasibility of transmitting CCSDS [3] conform telemetry via this link and to generate and introduce a real-time compressed video stream into this downlink data stream. Because these goals generated demanding requirements to the on-board computer (OBC) with respect to speed and I/O functionality, it was not possible to go by standard 8-bit or 16-bit Microcontrollers (e.g. ATMEL AVR series) but necessary to choose a high-performance system. In the end, the National Instruments SingleBoard RIO system was chosen. The main reason for this decision was the favorable combination of 2 Megagate Xilinix FPGAs, a PowerPC core with VX-Works real-time operating system and a multitude of onboard I/O.

2.2. Implementation Experience

The availability of an FPGA made it possible to break down the required functionality into high and low-level tasks of which the latter can be implemented very efficiently on the FPGA. Those parts of the software, including mission critical parts like the telecommand (TC) interface and state machine, could be parallelized and executed very fast. More complicated manipulations running at lower frequencies were executed on the real-time CPU. This scheme is depicted in Fig. 8.

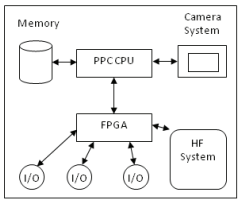

Figure 8: Space segment electronics architecture

Programming with LabVIEW turned out to be very fortunate, because it makes it easy for a team to develop various software components together and to achieve a satisfactory and common style level of documentation due to the nature of visual programming. The interaction between FPGA and CPU can especially be handled efficiently. But the limit of a maximum of three one-way communication channels (DMA FIFOs) between the two parts of the system required a thorough understanding of the required interfaces early in the development process.
Debugging possibilities, which are the most important in all phases of development, were also very good when working on software for one system at a time. Debugging the whole system can be very time intensive.
With growing complexity, it became obvious that the comfort described before has also costs, namely when it comes to optimizing performance on the CPU. Here, the LabVIEW layer between the actual operating system and the programmer prevents effective diagnosis and improvement actions. In the end, this resulted in a CPU load of only marginally below 100%, which is actually no figure for the CPU's real performance, but rather, the immense amount of overhead generated by LabVIEW programming.
Nevertheless, it should be emphasized that developing the whole OBC system for VECTOR in a visual programming environment was a real success as it enabled students mostly unfamiliar with embedded systems and microcontrollers to rapidly develop a well-working highly complex system.

3. FPGA-BASED REAL-TIME VIDEO COMPRESSION

For the real-time video compression onboard the REXUS 8 rocket, the CCSDS 122.0-B-1 standard [4] was used. This compression algorithm provides good compression rates and due to the standardization by means of CCSDS, it is especially suitable for space applications. The CCSDS 122.0-B-1 standard is based on the commercial JPEG2000 standard—only a few compression options are changed in order to allow a more efficient implementation of the algorithm in hardware. A hardware implementation is required to achieve real-time compression performance. Even high-performance state-of-the-art x86 CPUs are not capable to compress a video stream with a resolution of 640x480 pixels with a frame rate of 25 images per second or more with modern high-compression algorithms in real-time. For systems used in space, the power dissipation is an important issue. A hardware-accelerated compression system allows, in addition, for a dramatic reduction in power dissipation. For these two reasons, the on-board video compression for REXUS 8 was implemented. During the flight of REXUS 8, it was running on the low-power FPGA platform Spartan-3 from XILINX.
The CCSDS 122.0-B-1 algorithm can be divided into two main parts: The first part is a Discrete Wavelet Transformation (DWT), the second one is a Bit Plane Encoder (BPE). The DWT unit transforms the input image data into a representation that is more suitable for the following data reduction and compression stage, or the BPE unit. The complete data processing chain is depicted in Fig. 9. Both processing units are fully developed and implemented in VHDL and synthesized with the XST tool chain from XILINX.

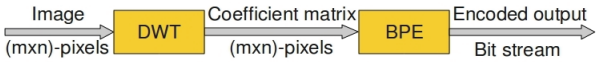

Figure 9: REXUS 8 video compressionsystem

The full video system is depicted in Fig. 10. As a video source, a commercial camera from JAI with a camera-link interface is used. For the connection to the FPGA an external camera-link adapter board is applied. An industrial micromodule FPGA board from Trenz-Electronic is used as a FPGA system.

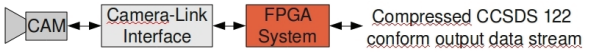

Figure 10: REXUS 8 video compression system

With the data rate available on the VECTOR S-band downlink of approx. 130kbits/s for the video data stream, the achieved frame rate was three frames per second, utilizing a compression rate of 0.128 (equals compressed/uncompressed image size).

4. CONCLUSIONS

Apart from the autonomous tracking, which represents the core of the VECTOR experiment, a real-time video compression algorithm based on a CCSDS standard was implemented. In order for the compressed images to be transmitted, an on-board data handling system was developed.

The video compression system was able to successfully demonstrate the capability of real-time video compression on a low-power Spartan-3 FPGA platform. Images were real-time compressed, sent down via the VECTOR S-band downlink and decompressed accordingly during the whole flight. Furthermore the chosen shared FPGA/Power PC OBC architecture programmed in LabVIEW allowed fast and effective implementation while meeting both CCSDS and real-time performance requirements.

An autonomous beam tracking method with a lightweight S-band antenna was implemented and could successfully be demonstrated on both REXUS 7 and 8 rocket flights. In general, the autonomous tracking worked very well. However, due to the chosen mechanism design, the antenna's agility was limited to 1.6Hz DST frequency, which is very small in comparison to other electronic conical tracking methods. Therefore, frequency overlaps during de-spin and reentry occurred, leading to several backup position resets (auto-track). Nevertheless, considering the used antenna's restricted capabilities, the fact of the mechanisms small North-misalignment on REXUS 7, the 30s posnet data dropout and diminutively defined step-size on REXUS 8, the overall tracking performance can be rated very positive. Future scenarios using this antenna and tracking method should, however, utilize a different antenna mechanism in order to manage increasing dynamic forces at high elevations. This could be realized by introducing an additional axis perpendicular to the azimuth and elevation axis. Thus, forces could be minimized resulting in a ten times higher agility of the antenna and therefore would allow to track faster moving objects and to evade the frequency overlap issue.

5. REFERENCES

1. R. Lundin et al. (2007), A compact and lightweight Inter-satellite antenna for S-Band, *The Second European Conference on Antennas and Propagation*, EICC, Edinburgh, UK
2. O. Persson et al. (2009), REXUS User Manual, Version 7.0, EuroLaunch
3. TM Space Data Link Protocol. Recommendation for Space Data System Standards, CCSDS 103.0-B-1. Blue Book. Issue 1 (2003), Washington, D.C.
4. Recommended Standard CCSDS 122.0-B-1 for Image Data Compression, including Technical Corrigendum 1 (2006), Washington, D.C.

6. ACKNOWDLEDGEMENTS

The authors would like to explicitly thank the German Aerospace Center (DLR) and the whole team from Esrange for their support within the REXUS sounding rocket program. With their financial support, *Bayrische Forschungsstiftung* as well as *Heinrich und Lotte Mühlfenzl-Stiftung* made it possible to conduct the research described in this paper. Furthermore, we would like to thank *Kayser-Threde*, *INTUS*, *LSE*, *Harmonic Drive, Trinamic* and *National Instruments* for their supply with high-tech hardware as well as valuable knowledge and experience.

The REXUS / BEXUS programme is realized under a bilateral Agency Agreement between the German Aerospace Center (DLR) and the Swedish National Space Board (SNSB). The Swedish share of the payload has been made available to students from other European countries through a collaboration with the European Space Agency (ESA). EuroLaunch, a cooperation between the Esrange Space Center of the Swedish Space Corporation (SSC) and the Mobile Rocket Base (MORABA) of DLR, is responsible for the campaign management and operations of the launch vehicles. Experts from ESA, SSC and DLR provide technical support to the student teams throughout the project. REXUS and BEXUS are launched from Esrange Space Center in northern Sweden.